Journal of Visualized Experiments

Dissection of Single Skeletal Muscle Fibers for Immunofluorescent and Morphometric Analyses of Whole-Mount Neuromuscular Junctions

--Manuscript Draft--

Article Type:	Invited Methods Article - Author Produced Video
Manuscript Number:	JoVE62620R2
Full Title:	Dissection of Single Skeletal Muscle Fibers for Immunofluorescent and Morphometric Analyses of Whole-Mount Neuromuscular Junctions
Corresponding Author:	Carmen Isabel Bolatto, Ph.D Universidad de la Republica Facultad de Medicina Montevideo, Montevideo URUGUAY
Corresponding Author's Institution:	Universidad de la Republica Facultad de Medicina
Corresponding Author E-Mail:	cbolatto@fmed.edu.uy
Order of Authors:	Carmen Isabel Bolatto, Ph.D
	Silvia Olivera-Bravo
	Sofía Cerri
Additional Information:	
Question	**Response**
Please specify the section of the submitted manuscript.	Neuroscience
Please indicate whether this article will be Standard Access or Open Access.	Standard Access ($1400)
Please confirm that you have read and agree to the terms and conditions of the author license agreement that applies below:	I agree to the Author License Agreement
Please provide any comments to the journal here.	
Please confirm that you have read and agree to the terms and conditions of the video release that applies below:	I agree to the Video Release

jove JOURNAL OF VISUALIZED EXPERIMENTS
1 Alewife Center #200
Cambridge, MA 02140
tel. 617.945.9051
www.jove.com

Standard Manuscript Template

TITLE:

Dissection of Single Skeletal Muscle Fibers for Immunofluorescent and Morphometric Analyses of Whole-Mount Neuromuscular Junctions

AUTHORS AND AFFILIATIONS:

Carmen Bolatto[1*#], Silvia Olivera-Bravo[2*], Sofía Cerri[1,2]

[1]Developmental Biology Laboratory, Histology and Embryology Department, Faculty of Medicine, Universidad de la República, Uruguay
[2]Cell and Molecular Neurobiology Laboratory, Clemente Estable Biology Research Institute (IIBCE), Ministerio de Educación y Cultura, Uruguay

*These authors contributed equally.

[#]IIBCE associated honorary researcher

Corresponding author:
Carmen Bolatto (cbolatto@fmed.edu.uy)

E-mail addresses of Co-Authors:
Carmen Bolatto (cbolatto@fmed.edu.uy)
Silvia Olivera-Bravo (solivera@iibce.edu.uy)
Sofía Cerri (scerrifassio@gmail.com)

KEYWORDS:
neuromuscular junction, skeletal muscle fiber, teased fiber, soleus, extensor digitorum longus, dissection, immunofluorescence, whole-mount, morphometric analysis.

SUMMARY:
The ability to accurately detect neuromuscular junction components is crucial in evaluating modifications in its architecture because of pathological or developmental processes. Here we present a complete description of a straightforward method to obtain high-quality images of whole-mount neuromuscular junctions that can be used to perform quantitative measurements.

ABSTRACT:
The neuromuscular junction (NMJ) is a specialized point of contact between the motor nerve and the skeletal muscle. This peripheral synapse exhibits high morphological and functional plasticity. In numerous nervous system disorders, NMJ is an early pathological target resulting in neurotransmission failure, weakness, atrophy, and even muscle fiber death. Due to its relevance, the possibility to quantitatively assess certain aspects of the relationship between NMJ components can help understand the processes associated with its assembly/disassembly.

The first obstacle when working with muscles is to gain the technical expertise to quickly identify and dissect without damaging their fibers. The second challenge is to utilize high-quality detection methods to obtain NMJ images that can be used to perform quantitative analysis. This article presents a step-by-step protocol for dissecting extensor digitorum longus and soleus muscles from rats. It also explains the use of immunofluorescence to visualize pre and postsynaptic elements of whole-mount NMJs. Results obtained demonstrate that this technique can be used to establish the microscopic anatomy of the synapsis and identify subtle changes in the status of some of its components under physiological or pathological conditions.

INTRODUCTION:

The mammal neuromuscular junction (NMJ) is a large cholinergic tripartite synapse made up of the motor neuron nerve ending, the postsynaptic membrane on the skeletal muscle fiber, and the terminal Schwann cells[1-3]. This synapse exhibits high morphological and functional plasticity[4-8], even during adulthood when NMJs can undergo dynamic structural modifications. For example, some researchers have shown that motor nerve endings continually change their shape at the micrometer scale[9]. It has also been reported that the morphology of the NMJ responds to functional requirements, altered use, aging, exercise, or variations in locomotor activity[4,10-15]. Thus, training and neglect represent an essential stimulus to modify some characteristics of the NMJ, such as its size, length, dispersion of synaptic vesicles and receptors, as well as nerve terminal branching[14,16-20].

Furthermore, it has been shown that any structural change or degeneration of this vital junction could result in motor neuron cell death and muscle atrophy[21]. It is also thought that altered communication among nerves and muscles could be responsible for the physiological age-related NMJ changes and possibly for its destruction in pathological states. Neuromuscular junction dismantling plays a crucial role in the onset of Amyotrophic Lateral Sclerosis (ALS), a neurodegenerative disease that constitutes one of the best examples of impaired muscle-nerve interplay[3]. Despite the numerous studies conducted on motor neuron dysfunction, it is still debated whether the deterioration observed in ALS occurs due to the direct damage into the motor neuron and then extends to the cortico-spinal projections[22]; or if it should be considered as a distal axonopathy where degeneration begins in the nerve endings and progresses toward the motor neuron somas[23-24]. Given the complexity of ALS pathology, it is logical to consider that a mix of independent processes occurs. As NMJ is the central player of the physiopathological interplay between muscle and nerve, its destabilization represents a pivotal point in the origin of the disease that is relevant to the analysis.

The mammal neuromuscular system is functionally organized into discrete motor units, consisting of a motor neuron and the muscle fibers that are exclusively innervated by its nerve terminal. Each motor unit has fibers with similar or identical structural and functional properties[25]. Motor neuron selective recruitment allows optimizing muscle response to functional demands. Now it is clear that mammalian skeletal muscles are composed of four different fiber types; some muscles are named according to the characteristics of their most abundant fiber type. For example, the soleus (a posterior muscle of the hind limb involved in the maintenance of the body posture) bears a majority of slow-twitch units (type 1) and is

recognized as a slow muscle. Instead, extensor digitorum longus (EDL) is essentially composed of units with similar fast-twitch properties (type 2 fibers) and is known as a fast muscle specialized for phasic movements needed for locomotion. In other words, although adult muscles are plastic in nature due to the hormonal and neural influences, its fiber composition determines the capacity to perform different activities, as seen in soleus that experiences continuous low-intensity activity and EDL that exhibits a more rapid single twitch. Other features that are variable among different types of muscle fibers are related to their structure (mitochondrial content, extension of sarcoplasmic reticulum, thickness of the Z line), myosin ATPase content, and myosin heavy chain composition[26-29].

For rodent NMJs, there are significant differences among muscles[28,29]. Morphometric analyses performed in soleus and EDL from rats revealed a positive correlation between the synaptic area and fiber diameter (i.e., the synaptic area in soleus slow fibers is greater than in EDL fast fibers) but the ratio between NMJ area and fiber size is similar in both muscles[30,31]. Also, in relation to the nerve terminals, the endplate absolute areas in type 1 fibers were lower than in type 2 fibers, whereas the normalization by fiber diameter made areas of nerve terminals in type 1 fibers the largest[32].

However, very few studies focus on morphometric analysis to show the evidence of changes in some of the NMJ components[33,34]. Thus, due to the relevance of the NMJ in the function of the organism, whose morphology and physiology are altered in various pathologies, it is important to optimize dissection protocols of different types of muscles with quality enough to allow the visualization of the whole NMJ structure. It is also necessary to evaluate the occurrence of pre or postsynaptic changes in different experimental situations or conditions such as aging or exercise[35-38]. In addition, it can be helpful to evidence more subtle alterations in NMJ components such as altered neurofilament phosphorylation in the terminal nerve endings as reported in ALS[39].

PROTOCOL:

All animal procedures were performed according to the guidelines of the National Law N° 18611 for Care of Animals Used for Experimental Purposes. The protocol was approved by the Institutional Ethical Committee (CEUA IIBCE, Protocol Number 004/09/2015).

1. Muscle dissection (Day 1)

NOTE: Before starting, make 40 mL of 0.5% paraformaldehyde (PFA), pH 7.4 in Dulbecco´s phosphate saline (DPBS). Optionally, make 20 mL of 4% PFA. Prepare 5 mL aliquots and freeze at -20 °C. On the day of dissection, defrost a 4% aliquot and add 35 mL of DPBS to obtain 40 mL of 0.5% PFA.

1.1. Isolation of EDL (fast-twitch muscle)

1.1.1. Euthanize a rat. Place the animal with the abdomen facing upwards. Make an initial incision using a surgical blade between the toes towards the hind limb.

NOTE: In this case, an intraperitoneal injection of 90:10 mg/Kg ketamine:xylazine was given to euthanize the rat, but other options of anesthesia are also allowed.

1.1.2. Peel off the skin, pulling it upwards until the rat knee is exposed.

1.1.3. To find the EDL, follow the foot tendons up to the annular ligament. This ligament circles two tendons. Cut the ligament between the two tendons with uniband scissors (or similar). Identify the EDL tendon by lifting both and choose the one that makes the toes move upwards.

1.1.4. Cut the tendon with uniband scissors. Then, while holding the tendon with fine biological tweezers, begin to slowly separate the EDL muscle from the tibialis anterior, the peroneus brevis, and peroneus longus[40] (see **Figure 1A**).

NOTE: Ensure that the muscle is separated without any damage. Do this by cutting the rest of the lateral muscles to open a path between them (the EDL does not have a superficial location) while holding and lifting the EDL muscle.

1.1.5. To completely isolate the muscle, cut the tendon attached to the rat knee with uniband scissors.

1.1.6. Immerse the dissected muscle in 5 mL of 0.5% PFA and leave for 24 h at 4 °C. Optionally, staple the muscle in a piece of cardboard and turn it with the muscle facing down. Then immerse it completely in 8 mL of the fixative solution. This step helps in maintaining the muscle elongated during the fixation process.

1.2 Isolation of soleus (slow-twitch muscle)

1.2.1 Flip the animal (the abdomen is now facing downwards). Through the skin, cut the calcaneal tendon using a surgical blade.

1.2.2. With the help of the biological tweezers and uniband scissors, separate the gastrocnemius muscle from the bones, creating a “muscular lid”. The soleus will be on the internal side of the muscular lid. It can be identified because it is red in color and has a flat morphology.

1.2.3. With a pair of biological tweezers, reach and lift the soleus tendon that lies above the gastrocnemius (see **Figure 1B**).

1.2.4. Cut the tendon with uniband scissors. Lift the whole muscle while cutting some of the weak attachment points (i.e., neurovascular elements). Finally, to completely free the soleus muscle, cut the soleus fascicle that forms the calcaneal tendon with uniband scissors.

1.2.5. Repeat step 1.1.6 to fix dissected soleus muscle.

2. Teased fiber preparation (Day 2)

2.1. After 24 h of fixation, rinse the muscles with 6 mL of DPBS solution 3x for 10 min each before isolating the muscle fibers.

2.2. To isolate the fibers, put a muscle on a microscope slide. Using a stereomicroscope, gently hold one of the tendons with one pair of biological tweezers. Then, with the other biological tweezers, begin to pinch the tendon slowly to separate the muscle fibers.

2.2.1. To isolate the fibers, slowly pull it upwards towards the opposite muscle tendon. It will be necessary to repeat this action several times until obtaining multiple small, isolated bundles.

2.3. Place them carefully on a pre-treated slide (silanized). It is necessary to keep all the fibers in order so that they do not overlap. At this point, air-dry the fibers for 24 h.

3. Immunofluorescence

3.1 Primary antibody incubation (Day 3)

NOTE: All steps were performed at room temperature, except if otherwise stated. The most efficient way to remove the different solutions without detaching fibers from the slide is to use an insulin syringe.

3.1.1. To start the immunostaining process, encircle the dried isolated muscle fibers with a pap pen to create a waterproof barrier.

3.1.2. To hydrate the muscle fibers, add 200 µL of distilled water for 5 min, and then change the water to 200 µL of DPBS for the next 5 min incubation. At this point, start the immunofluorescence labeling.

3.1.3. Incubate fibers with 300 µL of a blocking buffer (BB) containing 50 mM glycine, 1% BSA, and 1% Triton X-100 for 30 min.

3.1.4. Replace BB with the primary antibody at a concentration suggested by manufacturers. Use the BB to dilute the antibody. This experiment used 400 µL of SMI 32 or SMI 31 that recognized non-phosphorylated or phosphorylated neurofilament H at 1/800 dilution to detect the NMJ presynaptic component.

NOTE: When deciding to recognize the whole presynaptic element instead of evaluating neurofilament phosphorylation, choose antibodies against synapsin, synaptophysin or SV2a that were previously successfully employed.

3.1.5. Incubate the fibers with the primary antibody dilution at 4 °C overnight (optionally,

incubation can be performed at 37 °C for 1 h). In both cases, it will be important to perform the incubation using a humid chamber.

3.2. Immunofluorescence: Secondary antibody incubation (Day 4)

3.2.1. Remove the primary antibody and rinse the fibers 3x for 10 min each with 500 µL of DPBS and the last time with BB.

3.2.2. Remove this last wash and add the fluorescently labeled secondary antibody diluted in BB. For this experiment, 500 µL of goat anti-mouse Alexa Fluor 488 at 1/1000 dilution in BB was used. To view the postsynaptic element of the NMJs, 1:300 α-Bungarotoxin, biotin-XX conjugate was added to the secondary antibody dilution.

NOTE: The addition of XX-Btx allows better signal-to-noise images once detected with streptavidin that amplifies the signal. In addition, streptavidin conjugation to different fluorophores increased color combinations in co-labeling assays. Alternatively, fluorescently labeled Btx allows obtaining images of similar quality.

3.2.3. Incubate the secondary antibody and the Btx for 2 h at room temperature or 1 h at 37 °C protected from light.

3.2.4. Remove the secondary antibody and the Btx. Wash 3x for 10 min each with 500 µL of DPBS and the last rinse with BB.

3.2.5. Incubate with 500 µL of Streptavidin Alexa Fluor 555 at 1/1000 dilution with BB for 1 h at room temperature. At this point, if desired, add a probe to counterstain the nuclei, such as diaminophenylindole at a final concentration of 1 µg/mL.

3.2.6 Remove the incubation solution and wash fibers 3x for 10 min each with 500 µL of DPBS. Then, mount the fibers.

3.3. Mounting

3.3.1. Place 4 dots of transparent nail polish on the microscope slide as if they were the vertices of a square. Let them dry 1-2 min. These will be the points where the coverslips will rest, helping to avoid tissue crushing.

3.3.2. Remove the last DPBS wash and add enough mounting media (~ 200 µL) to cover the fibers; avoid drying.

NOTE: To prepare 10 mL of the mounting media mix, use Tris-HCl 1,5 M pH 8,8: glycerol in a 4:1 (v:v).

3.3.3. Use a 200 µL pipette tip to carefully spread the mounting media over the fibers to ensure

a complete immersion of all of them. Before placing the cover glass, remove air bubbles.

3.3.4. Place the coverslip onto the samples trying to prevent the generation of air bubbles. This movement can be done with the aid of forceps.

4. Microscopy and morphometric analysis

4.1. Image the teased fiber preparations using laser confocal microscopy.

4.2. Take a series of optical sections (30 µm Z stacks) across the entire synapse using a one-micrometer interval. To set the stack, use the Btx signal. Image at least 15-20 NMJs for each muscle condition with a 2048 px x 2048 px resolution. This method was chosen to obtain images with sufficient optical quality and resolution for the morphometric analysis.

4.3. To perform the measurements, use the projection images of stacks with any analysis software.

NOTE: Although the explained morphometric analysis was done manually, there are two recently developed Image J-based tools for studying many different aspects of pre and postsynaptic NMJ morphology[33,34].

4.4. To obtain the Total NMJ area values, select the external border (external outline of the stained area, see **Figure 2**) of the endplate using the **Magnetic lasso** tool and determine the number of selected pixels in the **Histogram** window. Then, the pixel areas can be converted to square micrometers using the scale specified by the confocal software.

4.5. With the same lasso tool, select the internal border (outlines of the stained area within the endplate, see **Figure 2**) and determine the non-stained area in the whole structure (or empty area) as detailed above (step 4.4.). The Postsynaptic Area values will be obtained after subtracting the total area from the empty area of each NMJ.

4.6. Obtain the Presynaptic Area, that is defined as the area with anti-neurofilament immunofluorescence, in a similar way that the Total NMJ area.

NOTE: All these parameters were used to determine the Post-Synaptic Density index (Postsynaptic Area/Total Area) and the NMJ Coverage (Presynaptic Area/Postsynaptic Area). A higher Postsynaptic Density index implies a denser -or more compact- endplate, whereas a smaller NMJ Coverage reflects a much poorer interaction between nerve terminal and endplate (both compatible with a denervation process). In the case shown here, since phosphorylated and non-phosphorylated forms of neurofilaments were detected at the nerve terminal level, the phosphorylated/non-phosphorylated presynaptic signal ratio and the phosphorylated/non-phosphorylated coverage ratio were calculated.

REPRESENTATIVE RESULTS:

This protocol offers a straightforward method to isolate and immunostain muscle fibers from two different types of muscles (fast- and slow-twitch muscles, see **Figure 1**). Using the correct markers and / or probes, NMJ components can be detected and evaluated since a quantitative point of view to assess some of the morphological changes that can occur as consequence of illness progression or a specific drug treatment. In the present study, presynaptic and postsynaptic components of the NMJ were fluorescently labeled using anti-neurofilaments (anti-Nf or anti-Phos-Nf) and alpha-bungarotoxin (Btx) respectively (**Figure 2**, upper panels). Each high-resolution confocal image of a NMJ obtained after the immunostaining was used to determine the morphometric measurements and indexes specified in the Protocol section (**Table 1**) applying the parameters described in the bottom panels of the **Figure 2**.

To demonstrate that this whole-mount NMJ preparation perfectly retained the synapse architecture, allowing the visualization of the effect that have a progressive nervous system disease on it, teased fibers of transgenic rats expressing human gene SOD1G93A (an ALS model) were immunostained using the protocol (**Figure 3**). The merging images of pre and postsynaptic signals with the nuclei stained with DAPI showed that differences among the NMJs between transgenic and non-transgenic age-matched animals are clearly visible and compatible with the results expected by literature.

In addition, the quality of images made it possible to quantify the changes observed by performing the morphometric analysis. For example, **Figure 4** shows evidence that the postsynaptic signal in transgenic animals appears to be more compact (approximately 20%), mainly due to the reduction of the NMJ total area.

On the other hand, **Figure 5** shows that the presynaptic area of the NMJs in transgenic animals is also reduced. The quality of this whole-mount NMJ preparation was evidenced by analyzing the extent of the nerve terminal retraction and by detecting changes concerning neurofilament phosphorylation states. This fact will be important to get a deep insight for the NMJ disassembly process related to ALS disease in the model employed. The smallest presynaptic area detected was the one labeled with anti-phosphorylated neurofilament (Figure 5 B, E, C, F).

The use of the coverage index (**Figure 6**) made it possible to establish that the transgenic NMJs were partially denervated. Also, it could determine that the coverage indexes of the phosphorylated neurofilament are lower than that obtained with non-phosphorylated neurofilament. These results show the pertaining to the status of whole-mount NMJ and that it could be useful to introduce the study of neurofilament phosphorylation state (an important determinant of filament plasticity and stability) using this whole-mount NMJ preparation.

Finally, methods presented in this work offer the greatest NMJ quality to identify, assess and evaluate even subtle changes in NMJ as a whole or in one of its component.

FIGURE AND TABLE LEGENDS:

Figure 1: EDL and soleus anatomical landmarks. Image highlight (**A**) EDL and (**B**) soleus location

among the other muscles of the rat lower hind limb. Insets show schemes of the hind limb muscles close to EDL (red) and soleus (green) muscles**.**

Figure 2: Whole-mount neuromuscular junction of EDL muscle fibers. (**A**) Postsynaptic component of NMJ detected using alpha-bungarotoxin (Btx, magenta), a probe that binds specifically to the acetylcholine receptors (AChR). (**B**) Motor terminal detected using anti-neurofilaments (anti-Nf, green). (**C,D**) Synaptic components are schematized in order to illustrate the parameters (external and internal borders) that defined the measurements (Total Area, Presynaptic and Postsynaptic Area) used for the morphometric analysis detailed in the protocol. Scale bar = 50 µm.

Figure 3: Pre and postsynaptic alterations observed in NMJs of an ALS model. Representative confocal images obtained from whole-mount NMJs obtained in preparations from EDL muscle fibers stained to detect neurofilaments (green), AChR (magenta), and nucleus (blue) from either non-transgenic (-/-) or transgenic (hSOD1G93A/-) rats. (**A,C**) Non-transgenic rats have normal NMJ morphology (pretzel shape) both when the motor end is visualized using anti-phospho neurofilament (Phos-Nf, A) or anti-neurofilaments (Nf, C). (**B,D**) Transgenic rats present more compact postsynaptic area and smaller presynaptic terminals with a reduction in the neurofilament phosphorylation signal. Scale bar = 50 µm.

Figure 4: Morphometric evaluation of the NMJ postsynaptic element in EDL muscles from 180 days old male hSOD1G93A rats. Representative confocal images of postsynaptic components in (**A,D**) non-transgenic and (**B,E**) transgenic animals. Evaluation of (**C**) postsynaptic area and (**F**) postsynaptic density index in NMJs of non-transgenic (solid columns) and transgenic (striped columns) animals. While the postsynaptic area was slightly reduced in transgenic animals, the postsynaptic index increased in greater proportion highlighting the degree of NMJ compaction as indicated by reduced total area in transgenic animals as shown in **Table 1**. Scale bar = 50 µm. Data represented is mean ± SEM (*) and (***) indicated $p<0.05$ and $p<0.001$, respectively.

Figure 5: Morphometric evaluation of the NMJ presynaptic element in EDL muscles from 180 days old male hSOD1G93A rats. Given the importance of NMJ disassembly in ALS disease, the quality of the preparation was evaluated by analyzing, not only the extent of the nerve terminal retraction, but also the possibility of detecting changes in the phosphorylation of the NMJ presynaptic element. Representative confocal images of the presynaptic component in (**A,D**) non-transgenic and (**B,E**) transgenic animals detected using (**A,B**) anti-phospho-neurofilament (Phos-Nf) or (**D,E**) anti-neurofilament antibodies (Nf). Evaluation of Presynaptic Area delimited by (**C**) phosphorylated and (**F**) non-phosphorylated neurofilaments in NMJs of non-transgenic (solid columns) and transgenic (striped columns) animals. Note that these areas are very similar in non-transgenic animals whereas they present a significant reduction in the NMJs of transgenic animals. Scale bar = 50 µm. Data represented is mean ± SEM ((****) indicated $p<0.0001$.

Figure 6: Evaluation of innervation status at whole-mount NMJs of EDL hSOD1G93A fibers. The coverage index is widely used to evaluate the state of innervation. It is considered that

"fully innervated" NMJs present a coverage index ≅50%, while those "partially innervated" have coverages between ≥20% and ≤50% and those vacant are considered "denervated". Representative confocal images of (**A,D**) non-transgenic and (**B,E**) transgenic NMJs showing presynaptic and postsynaptic elements detected using (**A,B**) anti-phospho-neurofilament (Phos-Nf) or (**D,E**) anti-neurofilament antibodies (Nf) to observe the motor terminal. Evaluation of coverage using (**C**) phosphorylated and (**F**) non-phosphorylated neurofilaments in NMJs of non-transgenic (solid columns) and transgenic (striped columns) animals. The images and graphics show evidence that NMJs from transgenic animals present a lower coverage index than non-transgenic ones. In addition, in transgenic animals, the coverage indexes of phosphorylated neurofilaments is lower (≅18%) than that obtained when the non-phosphorylated form (≅25%) is detected. This fact is corroborated with the relationship between both indexes as shown in **Table 1**. Note that the quality of the preparations allows obtaining ≅50% of the coverage index stipulated for the NMJs expected as "fully innervated". Scale bar = 50 μm. Data represented is mean ± SEM (***) and (****) indicated $p<0.001$ and $p<0.0001$, respectively.

Table 1. Morphometric parameters and ratios obtained from whole-mount NMJs of non-transgenic and transgenic EDL fibers.

DISCUSSION:

In this article, we present a detailed protocol for the dissection of two rat skeletal muscles (one slow-twitch and the other fast-twitch), fiber muscle isolation and immunofluorescence detection of pre and postsynaptic markers, and image quantitative analysis as a tool to study NMJ assembly/disassembly processes. This kind of protocol can be useful in rodent models[41, 42] to evaluate NMJ during physiological or pathological processes as exemplified here in a model of motor neuron degeneration such as found in the ALS hSOD1G93A rats.

To obtain success and beneficial results, it is necessary to keep in mind some tips. For example, the protocol described allows immediate use of dissected muscles. However, when necessary to preserve the muscle longer the use of DPBS with 0.05% sodium azide plus 4 °C storage allows prolonging excellent muscle preservation up to 4 weeks. When using this option, extensive washes with DPBS must be done (5x, 10 min each) before starting the staining process. Another helpful option to obtain good quality images includes lowering the PFA concentration at 0.5% because it reduced the muscle autofluorescence. This must be accompanied by longer fixation up to 24 h at 4 °C.

Regarding fiber isolation, smaller groups of fibers produce better immunodetection qualities. The fibers dried on silanized slides must be used within 2 to 3 days. After this time, the immunodetections are not of good quality.

One alternative to dried fibers on silanized slides is to generate a set of partially isolated fibers that are held together by the tendon tissue in one of the fibers end (a "tuft" of muscle fibers) and carry out incubations in microcentrifuge tubes by the "free-floating" method. Using this option is necessary to increase the antibody incubation times by several hours (24-48 h) as well as the number of washes (at least 6 of 10 min each).

In relation to fiber isolation without damage, it is necessary to perform the “tease” by removing the ends where the tendon is gently pull in opposite directions to achieve fiber separation.

Another critical step to improve immunodetection is the addition of 1% Triton X-100 and 50 mM glycine in the BB. This is important to obtain preparations that have homogeneous staining and a little background. It is also worth mentioning that having a little background can be beneficial when ordered, and unstained fibers need to be imaged. The fiber diameter is good to be measured far from the NMJ field since it is described that it may be increased at this level. Therefore, determine the fiber diameter at a distance equal to the value of an NMJ profile.

Using the procedure presented it is possible identifying and quantitating NMJ components under physiological conditions. It also allows studying early key pathological events as NMJ dismantlement[24] and loss of phosphorylated neurofilament in terminal endings[39] as described in ALS pathogenesis. For this reason, the protocol described offers an alternative and simple approach to help to get a better understanding of the NMJ remodeling, suggesting that morphological features visualized can be useful tools to diagnose degenerating state of NMJs or to assess different therapeutic approaches. It is also applicable to other disease models such as those of Charcot-Marie-Tooth[41] and spinal muscular atrophy[42] that present NMJ disruption.

In addition, approaches described in this work can be employed to identify the Schwann cells that integrate this tripartite synapse and eventually to assess some of its roles during NMJ remodeling[43]. Studies can be done in neonates until adults, under physiological conditions or as a response to different treatments impacting on the neuromuscular system.

Finally, in spite of the excellent handling needed to dissect and label samples together with time consumed to make manual measurements, methodology presented here enables an optimal labeling of the different NMJ components because of the facilitated penetration of antibodies and probes. Although better penetration can be obtained in sectioned muscle preparations, teasing preserves the 3D morphological integrity of all of the synaptic components that can be lost in muscle sections. It also avoids all of the preparation needed to make sections such as the inclusion of the muscle piece and further antigen retrieval to obtain feasible recognition. Furthermore, when compared to whole mount preparations that preserve the complete innervation patterns, teasing enables the study of isolated fibers. This can be a significant advantage when necessary to assess the fiber heterogeneity reported in pathological conditions.

ACKNOWLEDGMENTS:

Many thanks to CSIC and PEDECIBA for the financial support given to this work; to Natalia Rosano for her manuscript corrections; to Marcelo Casacuberta that makes the video and to Nicolás Bolatto for lending his voice for it.

DISCLOSURES:

The authors have nothing to disclose.

REFERENCES:

1. Araque, A., Parpura, V., Sanzgiri, R. P., Haydon, P. G. Tripartite synapses: Glia, the unacknowledged partner. *Trends Neuroscience.* **22**, 208–215 (1999).
2. Robitaille, R. Modulation of synaptic efficacy and synaptic depression by glial cells at the frog neuromuscular junction. *Neuron.* **21**, 847–855 (1998).
3. Cappello, V., Francolini M. Neuromuscular Junction Dismantling in Amyotrophic Lateral Sclerosis. *International Journal of Molecular Sciences* **18** (10), 2092-2108 (2017).
4. Deschenes, M. R., Tenny, K. A., Wilson, M. H. Increased and decreased activity elicits specific morphological adaptations of the neuromuscular junctions. *Neuroscience.* **137**, 1277-1283 (2006).
5. Desaulniers, P., Lavoie, P. A., Gardiner, P. F. Habitual exercise enhances neuromuscular transmission efficacy of rat soleus muscle in situ. *Journal Applied Physiology.* **90**, 1041-1048 (2001).
6. Deschenes, M. R., Roby, M. A., Glass, E. K. Aging influences adaptations of the neuromuscular junction to endurance training. *Neuroscience.* **190**, 56-66 (2011).
7. Valdez, G. et al. Attenuation of age-related changes in mouse neuromuscular synapses by caloric restriction and exercise*. Proceedings National Academy of Science U.S.A.* **107**, 14863-14868 (2010).
8. Arnold, A-S. et al. Morphological and functional remodeling of the neuromuscular junction by skeletal muscle PGC-1α. *Nature Communications*. **5**, 3569-3595 (2014).
9. Hill, R. R., Robbins N., Fang Z. P. Plasticity of presynaptic and postsynaptic elements of neuromuscular junctions repeatedly observed in living adult mice. *Journal of Neurocytology.* **20** (3), 165-182 (1991).
10. Brown, M. C., Hopkins, W. G., Keynes R. J., White J. A comparison of early morphological changes at denervated and paralyzed endplates in fast and slow muscles of the mouse. *Brain Research.* **248**, 382-386 (1982).
11. Rosenheimer, J. L. Effects of chronic stress and exercise on age related changes in end-plates architecture. *Journal of Neurophysiology.* **53**, 1582-1589 (1985).
12. Andonian, M. H., Fahim, M. A. Effects of endurance exercise on the morphology of mouse neuromuscular junctions during ageing. *Journal of Neurocytology.* **16**, 589-599 (1987).
13. Tomas, J., Fenoll, R., Santafé, M., Batlle, J., Mayayo E. Motor nerve terminal morphologic plasticity induced by small changes in the locomotor activity of the adult rat. *Neuroscience Letters.* **106**, 137-140 (1989).
14. Deschenes, M. R., Maresh, C. M., Crivello, J. F., Armstrong, L. E., Kramer, W. J., Covault, J. The effects of exercise training of different intensities on neuromuscular junction morphology. *Journal of Neurocytology.* **22**, 603-615 (1993).
15. Nishimune, H., Stanford, J. A., Mori, Y. Role of exercise in maintaining the integrity of the neuromuscular junction. *Muscle Nerve.* **49** (3):315-324 (2014)
16. Andonian, M. H., Fahim, M. A. Endurance exercise alters the morphology of fast- and slow-twitch rat neuromuscular junction. *International Journal of Sports Medicine*. **9**, 218-223 (1988).
17. Fahim, M. A. Endurance exercise modulates neuromuscular junction of C57BL\6N in ageing mice. *Journal of Applied Physiology.* **83**, 59-66 (1997).

18. Waerhaug, O., Dahl, H. A., Kardel, K. Different effects of physical training on morphology of motor nerve terminals in rat extensor digitorum longus and soleus muscles. *Anatomy and Embryology.* **186**, 125-128 (1992).
19. Desaulniers, M. R., Lavoie, P. A., Gardiner, P. F. Endurance training increases acetylcholine receptor quantity at neuromuscular junctions of adult rat skeletal muscle. *Neuroreport.* **9**, 3549-3552 (1998).
20. Deschenes, M. R. et al. Effects of resistance training on neuromuscular junction morphology. *Muscle Nerve.* **23**, 1576-1581 (2000).
21. Lepore, E., Casola, I., Dobrowolny, G., Musarò, A. Neuromuscular Junction as an Entity of Nerve-Muscle Communication. *Cells.* **8** (8), 906-921 (2019).
22. Braak, H. et al. Amyotrophic lateral sclerosis—A model of corticofugal axonal spread. *Nature Review Neurology.* **9**, 708–14 (2013).
23. Fischer, L. R. et al. Amyotrophic lateral sclerosis is a distal axonopathy: Evidence in mice and man. *Experimental Neurology*. **185**, 232-240 (2004).
24. Moloney, E. B., de Winter, F., Verhaagen, J. ALS as a distal axonopathy: molecular mechanisms affecting neuromuscular junction stability in the presymptomatic stages of the disease. *Frontiers in Neuroscience.* **14** (8), 252-270 (2014).
25. Scott, W., Stevens, J., Binder-Macleod, S. A. Human skeletal muscle fiber type classifications. *Physical Therapy*. **81**, 1810-1816 (2001).
26. Schiaffino, S., Hanzlíková, V., Pierobo, S. Relations between structure and function in rat skeletal muscle fibers. *Journal of Cellular Biology.* **47** (1), 107–119 (1970).
27. Schiaffino, S., Reggiani, C. Fiber types in mammalian skeletal muscles. Review. *Physiological Reviews.* **91** (4), 1447-1531 (2011).
28. Mech, A. M., Brown, A. L., Schiavo, G., Sleigh, J. N. Morphological variability is greater at developing than mature mouse neuromuscular junctions. *Journal of Anatomy* **237** (4), 603-617 (2020).
29. Jones, R. A. et al. NMJ-morph reveals principal components of synaptic morphology influencing structure-function relationships at the neuromuscular junction. *Open Biology*. **6** (12), 160240 (2016).
30. Waerhaug, O., Lømo, T. Factors causing different properties at neuromuscular junctions in fast and slow rat skeletal muscles. *Anatomy and Embryology.* **190**, 113-125 (1994).
31. Wood, S. J., Slater, C. R. The contribution of postsynaptic folds to the safety factor for neuromuscular transmission in rat fast- and slow-twitch muscles. *Journal of Physiology.* **500,** 165-176 (1997).
32. Prakash, Y. S., Miller, S. M., Huang, M., Sieck, G. C. Morphology of diaphragm neuromuscular junctions on different fibre types. *Journal of Neurocytology*. **25**, 88 –100 (1996).
33. Murray, L. M., Gillingwater, T. H., Parson, S. H. Using mouse cranial muscles to investigate neuromuscular pathology in vivo. *Neuromuscular Disorders*. **20** (11), 740-743 (2010).
34. Mejia Maza A. et al. NMJ-Analyser: high-throughput morphological screening of neuromuscular junctions identifies subtle changes in mouse neuromuscular disease models. *bioRxiv.* (2020).
35. Burke, S. R. A., Reed, E. J., Romer, S. H., Voss, A. A., Levator auris longus preparation for examination of mammalian neuromuscular transmission under voltage clamp conditions. *Journal of Visualized Experiments*. (135), e57482 (2018).

36. Franco, J. A., Kloefkorn, H. E., Hochman, S., Wilkinson, K. A. An in vitro adult mouse muscle-nerve preparation for studying the firing properties of muscle afferents. *Journal of Visualized Experiments.* (91), e51948 (2014).
37. Brill MS, Marinkovic P, Misgeld T. Sequential photo-bleaching to delineate single Schwann cells at the neuromuscular junction. *Journal of Visualized Experiments* (71) e4460, (2013).
38. Murray, L., Gillingwater, T. H., Kothary, R. Dissection of the transversus abdominis muscle for whole-mount neuromuscular junction analysis. *Journal of Visualized Experiments* (83), e51162 (2014).
39. Tsang, Y. M., Chiong, F., Kuznetsov, D., Kasarskis, E., Geula C. Motor neurons are rich in non-phosphorylated neurofilaments: cross-species comparison and alterations in ALS. *Brain Research*. **861** (1), 45-58 (2000).
40. Balice-Gordon, R. J., Thomposon, W. J. The organization and development of compartmentalized innervation in rat extensor digitorum longus muscle. *Journal of Physiology*. **398**, 211-231 (1988).
41. Cipriani, S. et al. Neuromuscular junction changes in a mouse model of Charcot-Marie-Tooth disease type 4C. *International Journal of Molecular Science*. **19** (12), 4072 (2018).
42. Boido, M., Vercelli, A. Neuromuscular junctions as key contributors and therapeutic targets in spinal muscular atrophy. *Frontiers in Neuroanatomy*. **10**, (6), (2016).
43. Barik, A., Li, L., Sathyamurthy, A., Xiong, W-C., Mei, L. Schwann cells in neuromuscular junction formation and maintenance. *Journal of Neuroscience*. **36** (38), 9770–9781 (2016).

Figure

Click here to access/download;Figure;Figura 1_JoVE62620.psd

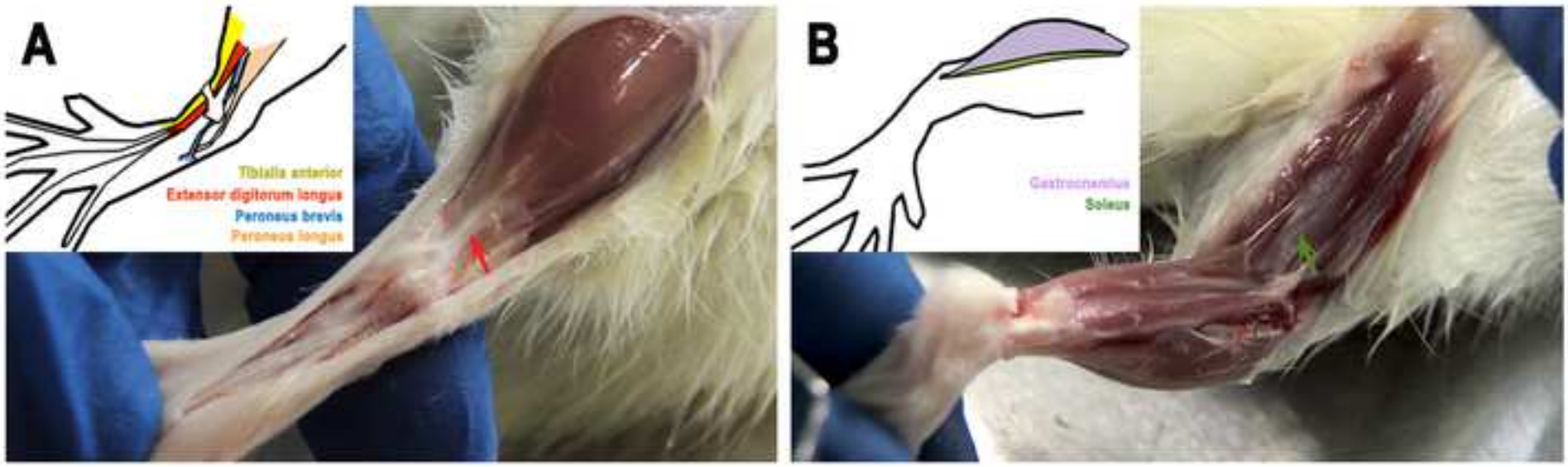

Figure

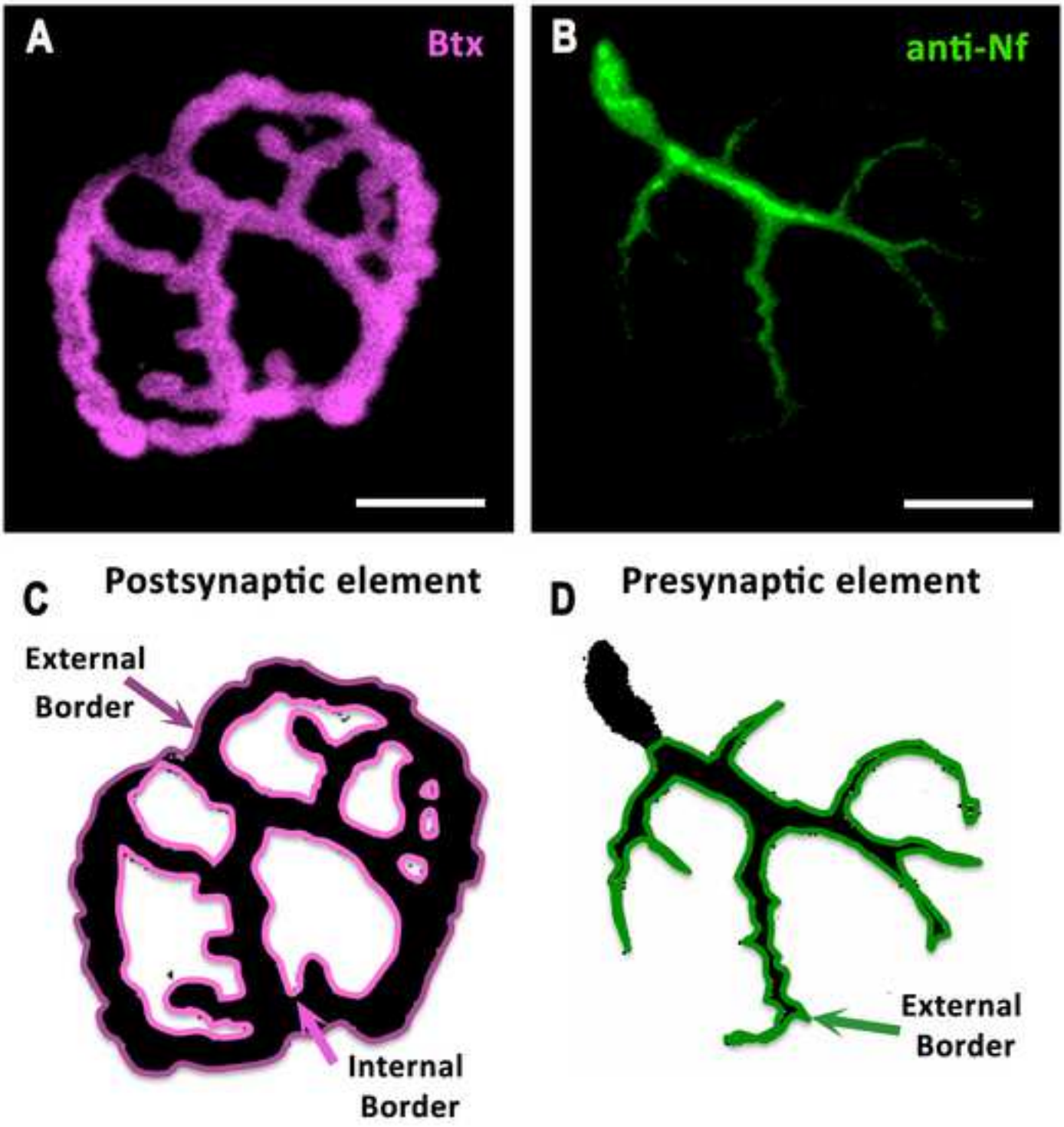

Figure

Click here to access/download;Figure;Figure 3_JoVE62620.psd

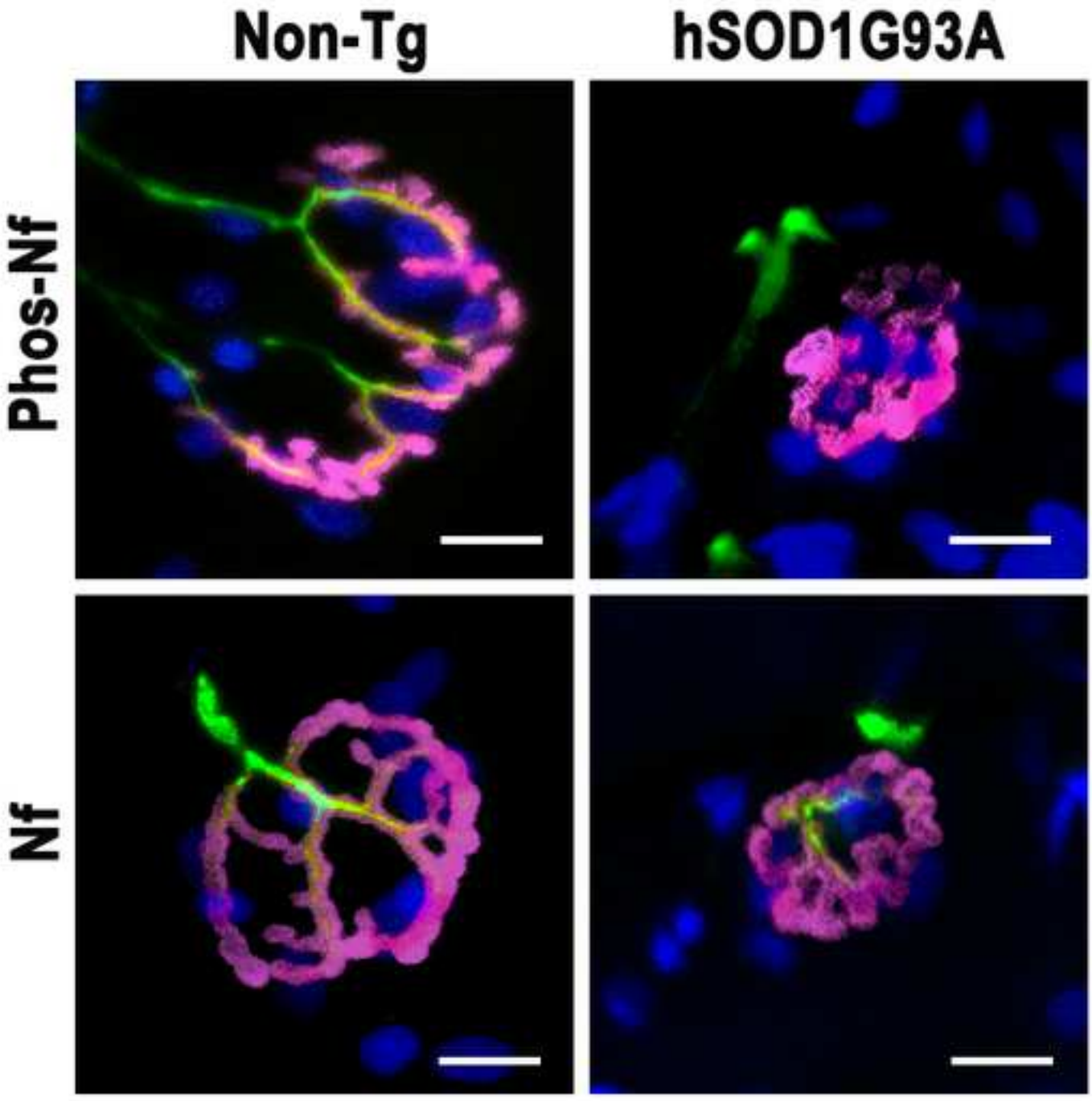

Figure

Click here to access/download;Figure;Figure 4_JoVE62620.psd

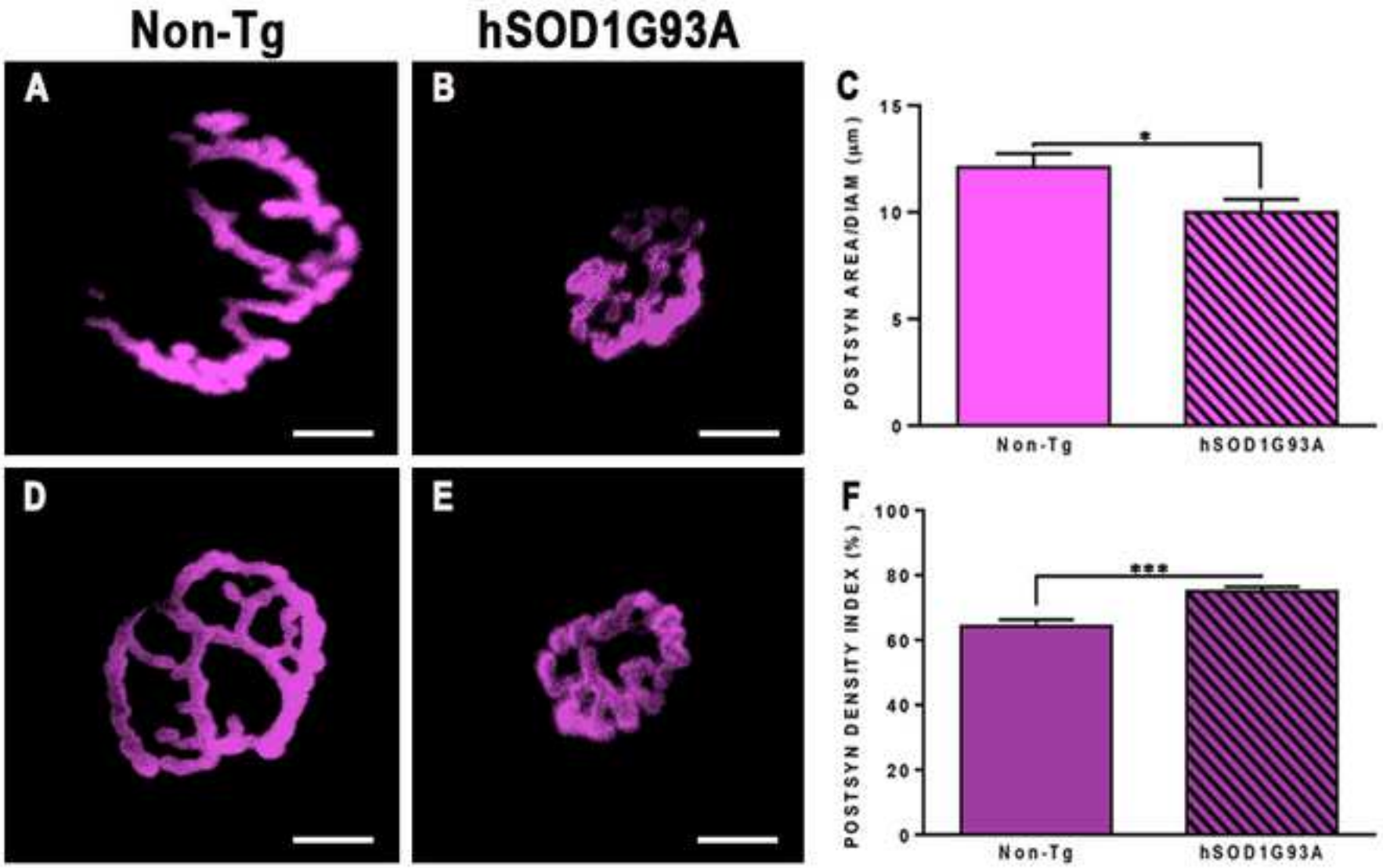

Figure

Click here to access/download;Figure;Figure 5_JoVE62620.psd

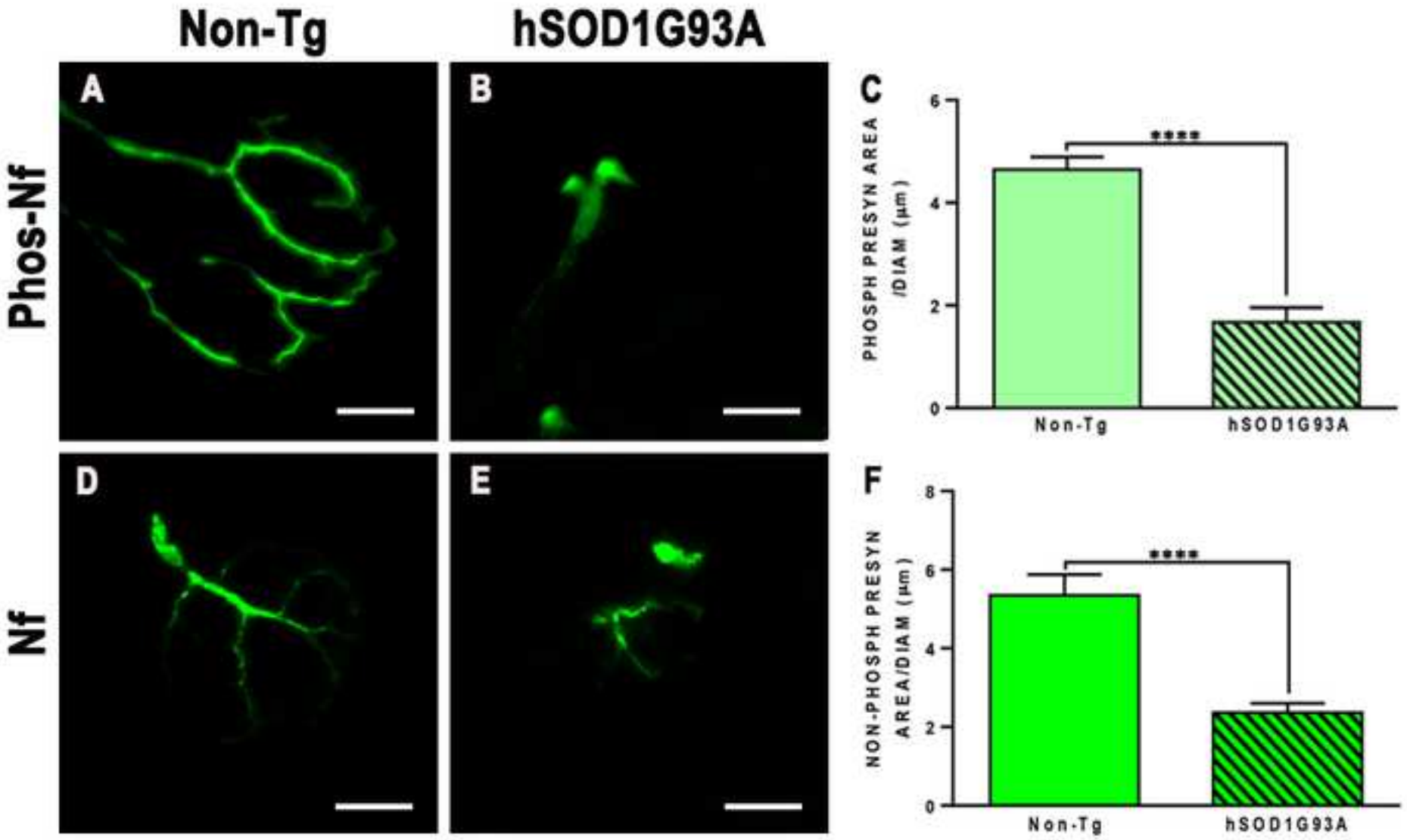

Figure

Click here to access/download;Figure;Figure 6_JoVE62620.psd

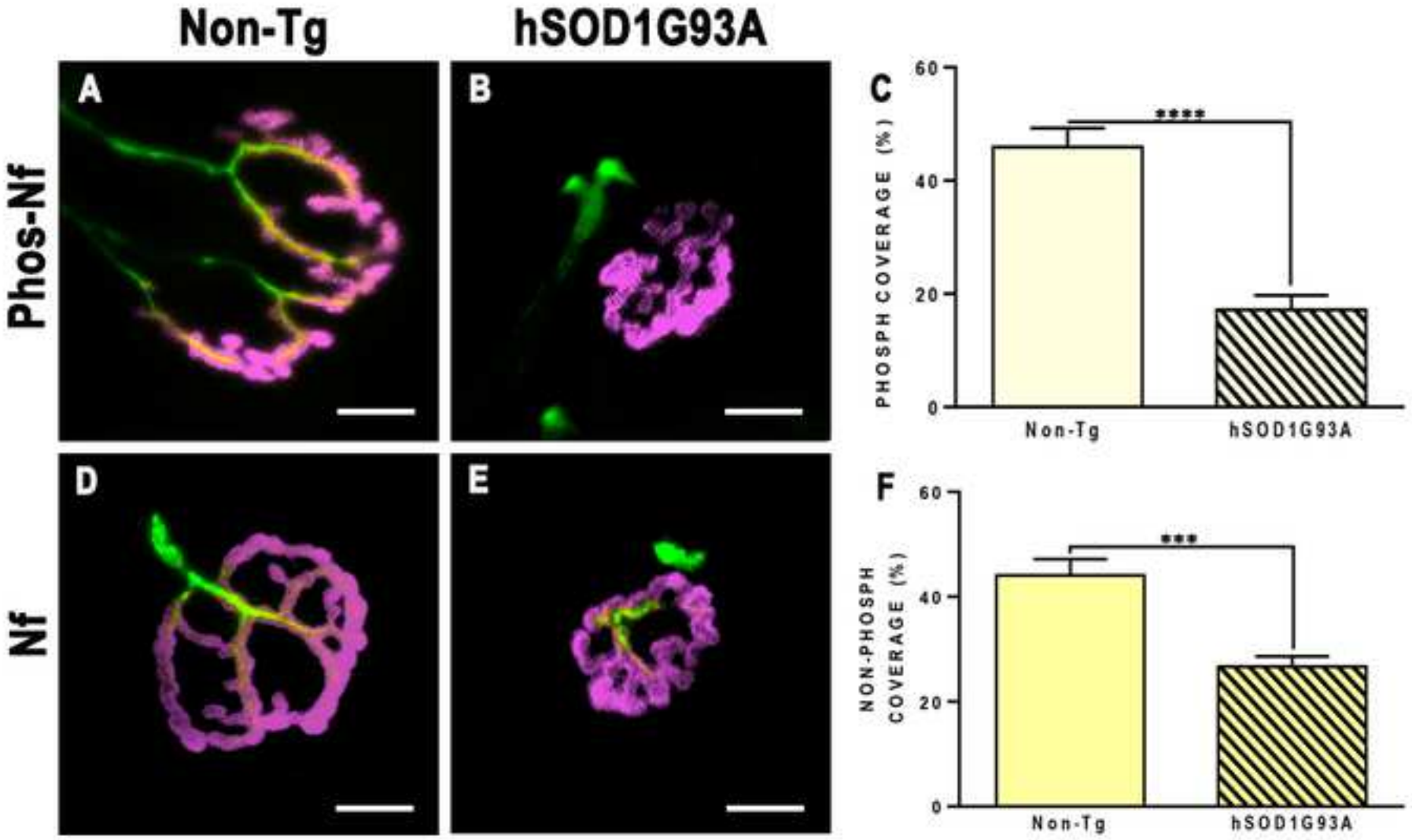

Parameters and Ratios	***Non-Tg***	***hSOD1G93A***	***Statistics***	***p value***
Fiber Diameter (µm)	49,35±2,65	51,36±2,11	n.s.	p=0,506
Non-Phosph Presyn Area/Diam (µm)	5,35±0,53	2,36±0.24	****	p<0,0001
Phosphorylated Presyn Area/Diam (µm)	4,65±-0,25	1,67±0,29	****	p<0,0001
Non-Phosph-Phosph Presyn Area (%)	100,0±21,1	45,25±8,44	**	p=0,0083
Postsyn Area/Diam (µm)	12,11±0,64	9,99±0,62	*	p=0,0152
Phosph Coverage (%)	45,93±3,35	17,17±2,54	****	p<0,0001
Non-Phosph Coverage (%)	44,06±3,14	26,69±1,93	****	p<0,0001
Phosph/Non-Phosph Coverage Ratio	1.37±0,19	0,61±0,11	****	p<0,0001
Total NMJ Area/Diam (µm)	18,73±1,22	14,56±0,86	**	p=0,0057
Postsyn Density Index (%)	64,28±0,98	75,03±1,47	***	p=0,0002

Values are means ± SEM

(*), (**), (***) and (****) denoted statistical significance with $p<0.05$, $p<0.01$, $p<0.001$ and $p<0.0001$, respectively.

n.s not significant.

June 17th, 2021

Dear. Dr. Vineeta Bajaj,

Firstly, we would like to thank you for reading our manuscript and reviewing it, which helped us to improve it again. We have revised our manuscript and made all the changes suggested. In this letter we have shortly addressed the answers to your comments. We have sent the revised manuscript containing all the modifications in track changes. Our response was typed in bold and italic font, directly beneath of each of your questions.

Best regards,

Carmen Bolatto, PhD

Editorial comments:

Changes to be made by the Author(s) regarding the written manuscript:

1. The editor has formatted the manuscript to match the journal's style. Please retain and use the attached file for revision.

R- Thanks to the editor. Manuscript format was retained.

2. Please address all the specific comments marked in the manuscript.

R- All the specific comments marked in the manuscript were addressed.

Regarding the change of the title, we would like to clarify that we try to adjust it to the recommendation that you gave us in comment 2 of the manuscript. As we feel that your recommendation may not reflect the real meaning of the title, we reworded it to: "Dissection of Single Skeletal Muscle Fibers for Immunofluorescent and Morphometric Analyses of Whole-Mount Neuromuscular Junctions ". This change was made in the video as well.

3. Once done please proofread the manuscript well.

R- The manuscript was proofread.

Changes to be made by the Author(s) regarding the video:

1. Please increase the homogeneity between the video and the written manuscript. Ideally, all figures in the video would appear in the written manuscript and vice versa. The video and the written manuscript should be reflections of each other.

R- Figure 1 was added to the text as requested from a reviewer. The video widely shows the muscle dissection, so adding it would be redundant (we consulted and the editor agreed with us). The rest of the figures of the text are in the video as well as all the main changes.

2. Still the Audio Levels are High and not Balanced. Please ensure audio level peaks average around -9 dB.

R- The video creator verified that the level of background music was at -30 dB and the average of the locution voice was at -9 dB.

3. 08:03 - 08:06 Please remove the background sound (Like inhaling Sound)

R- The background sound was removed.